A Systematic Study of Methyl Carbodithioate Esters as Effective Gold Contact Groups for Single-Molecule Electronics

Jonathan S. Ward *[a,b], Andrea Vezzoli [a], Craig Robertson [a], Richard J. Nichols *[a], and Simon J. Higgins[a]

[a] Department of Chemistry, University of Liverpool, Crown St., Liverpool, L69 7ZD, UK

[b] Chemistry Department, Lancaster University, Bailrigg, Lancaster, LA1 4YB, UK

E-Mail: nichols@liverpool.ac.uk, j.ward10@lancaster.ac.uk

Abstract

Currently, there is an array of binding groups for use within molecular electronics for anchoring molecules to metal electrodes (e.g., R–SMe, R–NH_2, R–CS_2^-, R–S^-). The problem is that some anchoring groups that bind strongly to electrodes have poor/unknown stability, or they have weak electrode coupling. More binding groups are required for molecular design with good stability and strong binding to the electrodes. Here, we present an in-depth investigation into the use of carbodithioate esters as contact groups for single-molecule conductance measurements, using scanning tunnelling microscopy break junction measurements (STM-BJ). We demonstrate using a series of novel molecular wires that the methyl carbodithioate ester acts as an effective contact for gold electrodes in STM-BJ measurements without deprotection. Surface enhanced Raman measurements demonstrate that the C=S functionality remains intact when adsorbed on to gold nanoparticle surfaces. A gold(I) complex was also synthesised showing a C=S→Au^I interaction highlighting that the ester remains intact while binding to a gold centre. Comparison with a benzyl thiomethyl ether demonstrates that the C=S significantly contributes to charge transport in single-molecule junctions. The synthetic accessibility and performance of the functional group reported here demonstrates that it should be used more extensively and has strong potential for the fabrication of larger area devices with long-term stability.

Introduction

Our understanding of how to design molecules that efficiently conduct electricity across a nanogap in a molecular junction (metal-molecule-metal) configuration has increased dramatically in the past 15 years.[1-7] The contact groups are a fundamental part of the design of molecular wires, providing mechanical and electronic coupling of the molecular species to the electrodes. The same molecular backbone can show remarkably different conductance profiles with different electrode contact groups,[8] and a deeper understanding of this behaviour requires substantial further study, for instance through the characterisation of wider libraries of regularly used contact groups. Thiol contact groups have been used extensively in molecular electronics due to their high affinity for gold surfaces and the strong, covalent Au–S bond formed following surface interaction (of energy easily surpassing 1 eV).[9-12] Thiol-based

molecules are particularly effective for monolayer fabrication, with the strong Au-S surface binding promoting the diffusion of gold atoms across the substrate surface.[13,14] Thiol contact groups can however be problematic for scanning tunnelling microscopy break junction (STMBJ) measurements, particularly under air, due to potential oxidation of the sulfur contact groups (among a number of other unwanted side reactions such as disulfide formation), and multiple anchoring configurations.[15] Thioether contact groups have been an excellent alternative contact group for gold substrates owing to their increased chemical stability, reasonable Au binding strength (0.5 – 0.8 eV) and preference for binding to undercoordinated Au atoms.[16] The main thioether contact groups that been used are methyl thioether[17-19] and benzodihydrothiophene.[19-22] While thioether contacts maintains good binding strength to gold, the coupling to the electrodes is not as efficient as with thiols due to the dative vs. covalent bond formed. Less efficient group electrode coupling can also be observed with other coordinating contact groups, such as pyridyl and amine.[20,23] Therefore, to further advance molecular electronics it would be highly advantageous to have additional contact groups that provide chemical stability, strong coupling to the electrodes, and ease of synthesis. We have been particularly interested in the use of carbodithioate esters as Au contact groups for single-molecule conductance measurements. This functionality has been investigated previously by Bourget and co-workers where the 2-(trimethylsilyl)ethyl ester moiety was used as a protecting group for a carbodithioate ($R–CS_2^-$) contact group,[24] but the single-molecule conductance of pristine carbodithioate ester (*i.e.* without deprotection to the anionic species) has not been investigated. Since these initial investigations on $R–CS_2^-$, there has been a proliferation in the use of STM-BJ instrumentation collecting large datasets and relying on good surface anchoring groups to achieve high quality electrical characterisation. Since there could be concerns around the stability of carbodithioate anion functionality due to similar possible issues experienced with thiol contact groups, we postulated that carbodithioate esters themselves could act as effective gold contacts without the need for deprotection. A carbodithioate methyl ester could retain the S–Me functionality that grants chemical stability to thioethers and the C=S functionality could provide additional coupling strength making it highly appealing for further investigations. As a result, we have synthesised a series of molecular wires with $R–CS_2Me$ contact groups in order to verify their suitability for the fabrication of electrically transparent, strong, and stable molecular junctions. The work demonstrates that carbodithioate esters are effective contact groups for molecular electronics with high junction formation probabilities even at low μM solution concentrations (Figure S24). Selected studies demonstrate long-term stability of the $R–CS_2Me$ functionality in the solution state under ambient conditions. Control experiments demonstrate that the presence of the C=S functionality compared to the benzyl methyl thioether equivalent boosts the conductance by approximately one order of magnitude. Further investigations, involving Raman studies and complexation with Au(I) salts, show that carbodithioate esters in the molecular wires prepared remain intact when on the gold surface. We also show that terminating molecular wires with the carbodithioate methyl ester functionality is synthetically accessible through Pd-catalysed cross-

coupling reactions. This work clearly demonstrates that carbodithioate esters are a useful functionality, likely to become a commonly used motif as part of a molecular electronics toolbox.

Results and discussion

Molecular design and synthesis

This work initially required the development of a series of molecular wires containing carbodithioate ester functionality that would enable detailed study of the contact group in STM-BJ experiments in addition to surface characterisation (**Figure 1**).

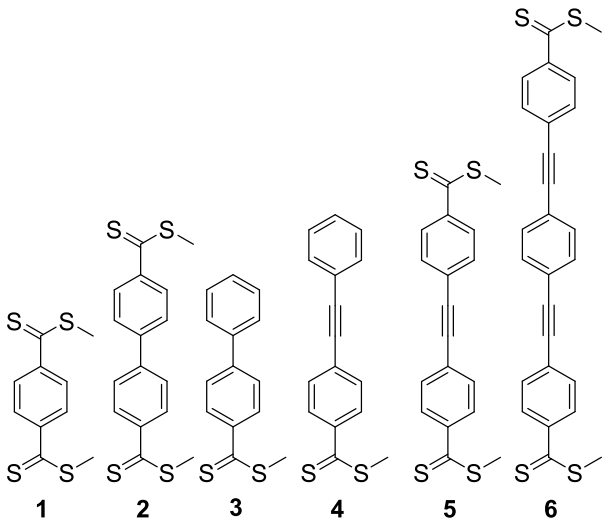

Figure 1. Carbodithioate ester containing molecular series prepared in this work.

The series in **Figure 1** contains molecular wires of varying molecular length with two carbodithioate ester groups for STM-BJ measurements (**1**, **2**, **5** and **6)**, and mono-carbodithioate ester functionality (**3** and **4**) for surface Raman measurements. **Scheme 1** shows an example synthetic strategy used to prepare alkyne-containing molecular wire **5**.

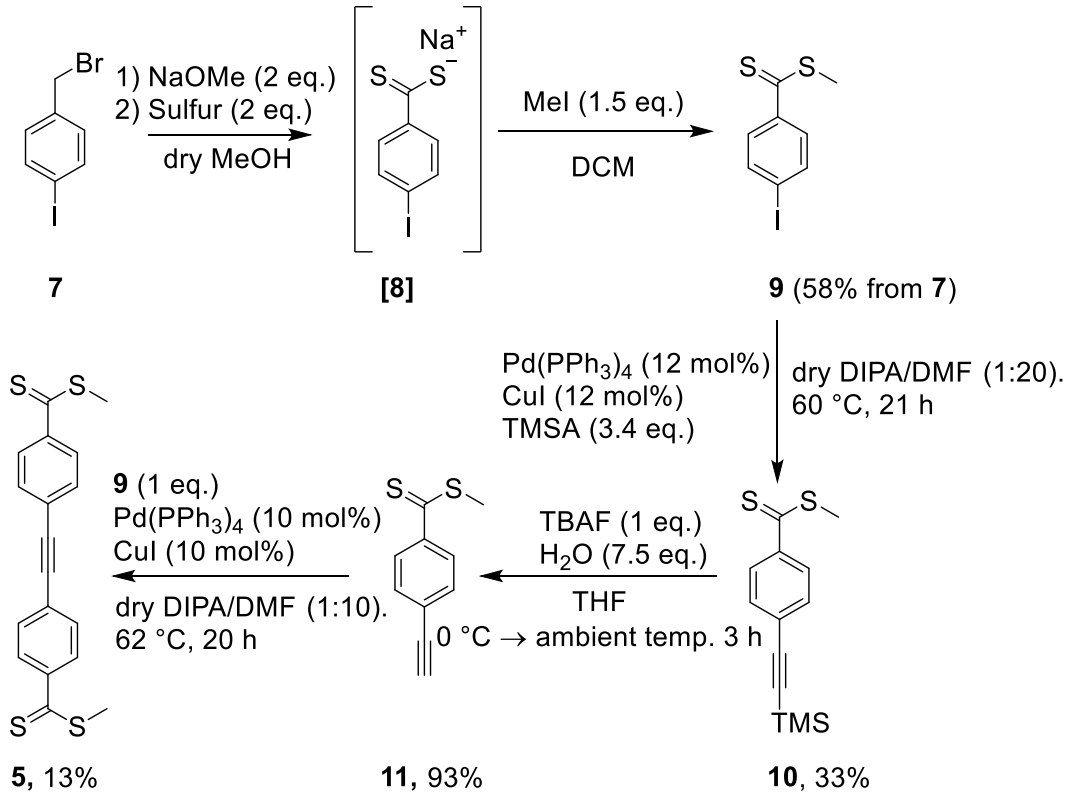

Scheme 1. Synthetic pathway to alkyne-containing molecule wire **5**.

Sodium carbodithioate functionality in this work was installed by treatment of benzyl halides with NaOMe (prepared *in-situ* by treating methanol with Na metal) and elemental sulfur.[25] Sodium intermediate **[8]** was treated with MeI in DCM to give the carbodithioate ester **9**. To make **5**, terminal alkyne-containing **11** was required for the appropriate Sonogashira cross-coupling with **9**. **11** was prepared by Sonogashira coupling of **9** with trimethylsilyl acetylene (TMSA) and subsequent deprotection with TBAF. The final Sonogashira coupling to yield **5** was performed using conditions reported by Querner and co-workers, which is one of the few reported cross-coupling transformations to tolerate the CS_2Me functionality.[26] Similar conditions were used to prepare the other carbodithioate ester-containing compounds in the series as detailed in the supporting information.

Scanning Tunnelling Microscopy-Break Junction Measurements.

The conductance of carbodithioate esters **1**–**2**, and **5**–**6** were measured using STM-BJ measurements in an anisole solution of the target molecular wire. (**Figure 2**).[27] In this technique, molecular junctions are fabricated between an Au tip and an Au substrate in a scanning tunnelling microscope. A bias is applied across the junction and the current is monitored as a function of the distance between the two electrodes. Details about the technique and the instrumentation used can be found in our previous publications on the subject.[28] For the measurement of the compounds presented in this study, relatively low concentrations (≤10 μM) were required to consistently acquire high quality data. A piezo ramp of 20 nm was required to continuously refresh the tip during extension and retraction cycles of the STM-BJ

measurement. 5000 traces were acquired for each target compound to obtain a statistically significant distribution of conductance data, analysed in the form of 1D histograms and 2D density maps (*vide infra*). Occasional manual piezo control pushing the tip 50–100 nm in to the surface was required to "clean" the tip. It is possible that at concentrations ≥ 100 μM, surface coverage with organic molecular wire occurs very rapidly, and this could explain why it is difficult to obtain single molecule junctions at these higher concentrations. Anisole was found to be an excellent solvent for measuring these molecules following difficulty in mesitylene and mesitylene:tetrahydrofuran mixtures (the large proportion of tetrahydrofuran needed resulting in etching of the Au substrate).[29]

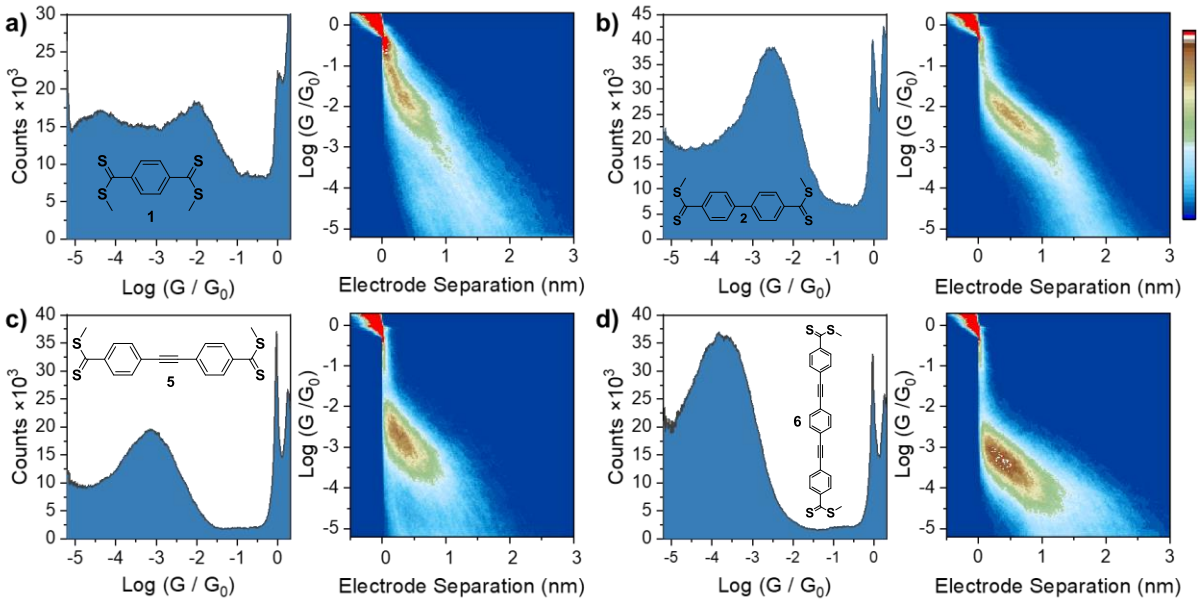

Figure 2. Scanning Tunnelling Microscopy Break-Junction measurements for a) **1,** b) **2**, c) **5** and d) **6** in anisole solvent at 10 μM for **1**–**2** and 1 μM for **5**–**6**. Further details: 300 mV bias, 20 nm piezo ramp.

STM-BJ results in **Figure 2** clearly show the value of carbodithioate esters as effective anchors to the gold electrodes. Clear conductance peaks are observed in the 1D histograms with high counts at the peak centre, and the 2D histograms demonstrate good general agreement of junction elongation with molecular length.. Compound **2** shows junction elongation beyond the theoretical S…S length at high concentration, (**Figure S23** in SI). Measurement at 1 μM is in better agreement with the molecular length. It is possible that with **2**, a small proportion of traces extend beyond the molecular length due to intermolecular stacking, thereby forming supramolecular 1:1 complexes of greater length. Compound **1** was also challenging to measure due to the short molecular length relative to the gold snapback distance and could only be measured at 10 μM; higher/lower concentrations failed to yield sufficiently high-quality traces. Compounds **5**–**6** had to be measured at 1 μM to collect the 5000 traces required. Being able to collect the data for **5**–**6** at such low concentrations further highlights the high affinity of the carbodithioate ester functionality for the Au surface.

Compound **12** (**Figure 3**) was also prepared to provide a direct comparison with molecule **2** to evaluate the benefit of adding C=S functionality. **12** was selected for comparison because of the comparable molecular length to **2**. STM-BJ measurements of **12** shows two overlapping conductance peaks at $10^{-3.64}$ and $10^{-4.05}$ (**Figure 3**) with a very clean break off in very good agreement with the molecular length. It is suggested that **12** shows two conductance peaks due to the degree of rotational flexibility in the molecule around the benzyl CH_2 positions. The presence of the C=S in **2** reduces the degrees of freedom, returning a clear, monodistributed conductance profile, and boosts the conductance compared to **12** by approximately an order of magnitude.

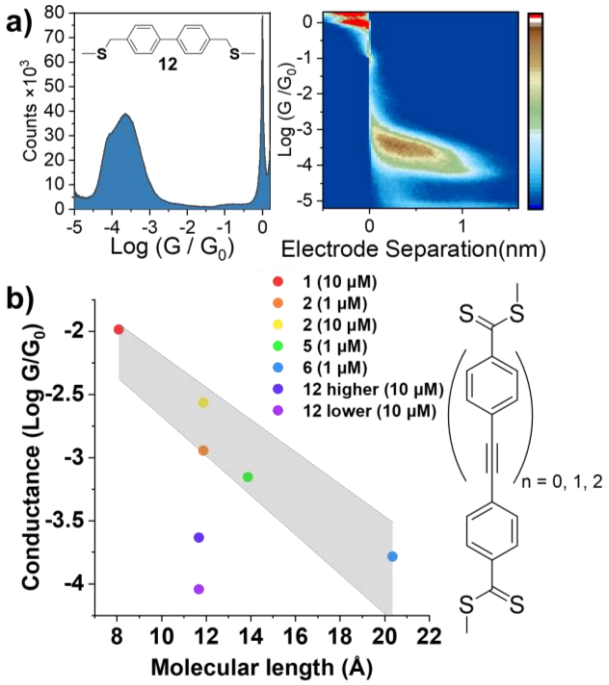

Figure 3. a) STM-BJ measurements of **12** at 300 mV bias in anisole at 10 μM. 20 nm piezo ramp. b) Conductance vs. molecular length for molecules measured in STM-BJ in anisole solvent at 300 mV bias. Linear fit of compounds **1**,**5** & **6** with ± 10% margin gives the grey shade area. Linear fit of **1**,**5**, & **6** used to calculate β value (β = 0.327)

The plot of log(conductance) vs. molecule length shows a clear linear trend for the carbodithioate ester-containing molecule wires. For the quasi-oligomeric series (**1**,**3**,**5**,**6**, see **Figure 3b**) it was not possible to measure the series at the same concentration due to the difficulties in measuring **1**, where 10 μM was the only concentration identified where 5000+ traces could be obtained. A ±10% margin of the linear fit of conductance for **1**, **5** & **6**, was used to demonstrate the general trend of conductance vs. molecular length. A β value of 0.327 $Å^{-1}$ for the linear fit is in reasonable agreement with data obtained in molecule wires with similar conjugated backbones.[20] The two conductance peaks for molecule **12** fall well outside of the shaded conductance trend for the carbodithioate esters, highlighting how the C=S moiety is significantly involved in electrode contact and charge transport, by providing additional electronic coupling between the molecule and the metallic electrodes.

Table 1 Conductance values for carbodithioate esters measured in anisole at 300 mV.

Entry	Conductance Log (G/G_0)
1 (10 μM)	−1.99
2 (10 μM)	−2.57
2 (1 μM)	−2.95
5 (1 μM)	−3.16
6 (1 μM)	−3.79
12 (10 μM) upper	−3.64
12 (10 μM) lower	−4.05

Stability study

To investigate the longer-term stability of the carbodithioate ester functionality, **1** was dissolved in DCM-d_2 and the ^{1}H NMR spectrum was acquired, followed by reacquisition after 13 days (**Figure 4**). In DCM-d_2, **1** remains stable in solution in the presence of oxygen and trace H_2O. This further highlights the benefits of using this functional group, where impurities in solutions of the substrates do not build up over relevant timeframes.

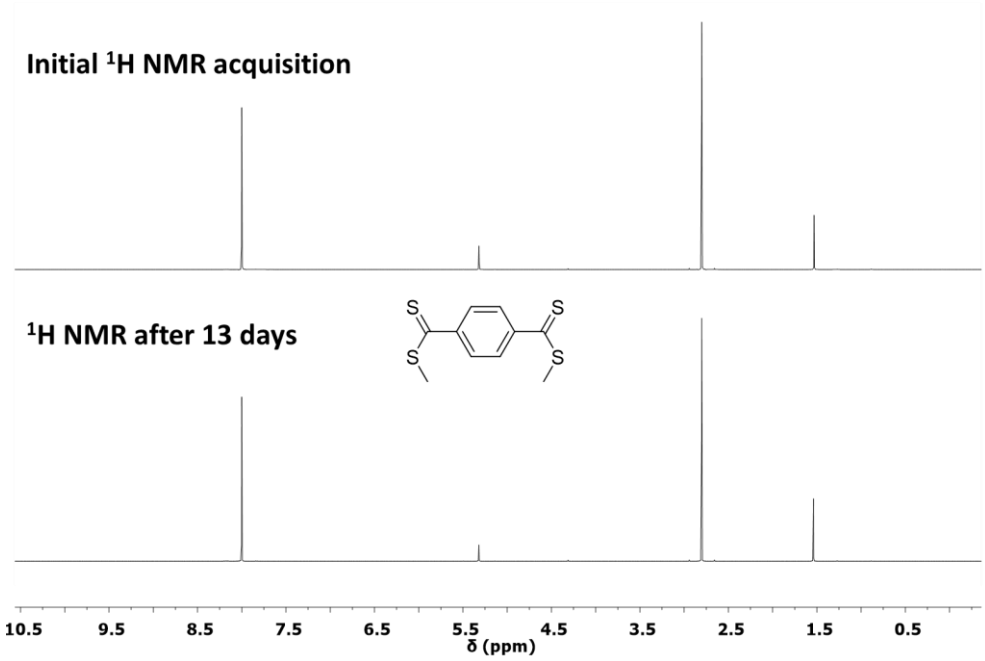

Figure 4 ^{1}H NMR of **1** in DCM-d_2 at 298 K after 0, and 13.05 days.

Surface Enhanced Raman Spectroscopy (SERS) measurements

To further demonstrate that the carbodithioate esters are clearly interacting with the surface, Raman measurements were performed on powder samples and compared with results from Surface-Enhanced Raman Spectroscopy (SERS) results, acquired from citrate capped gold nanoparticles (CitAuNP, prepared using literature procedure[30]) on silicon substrates where the molecule of interest was drop-casted from a 1 mM toluene solution (**Figure 5**).

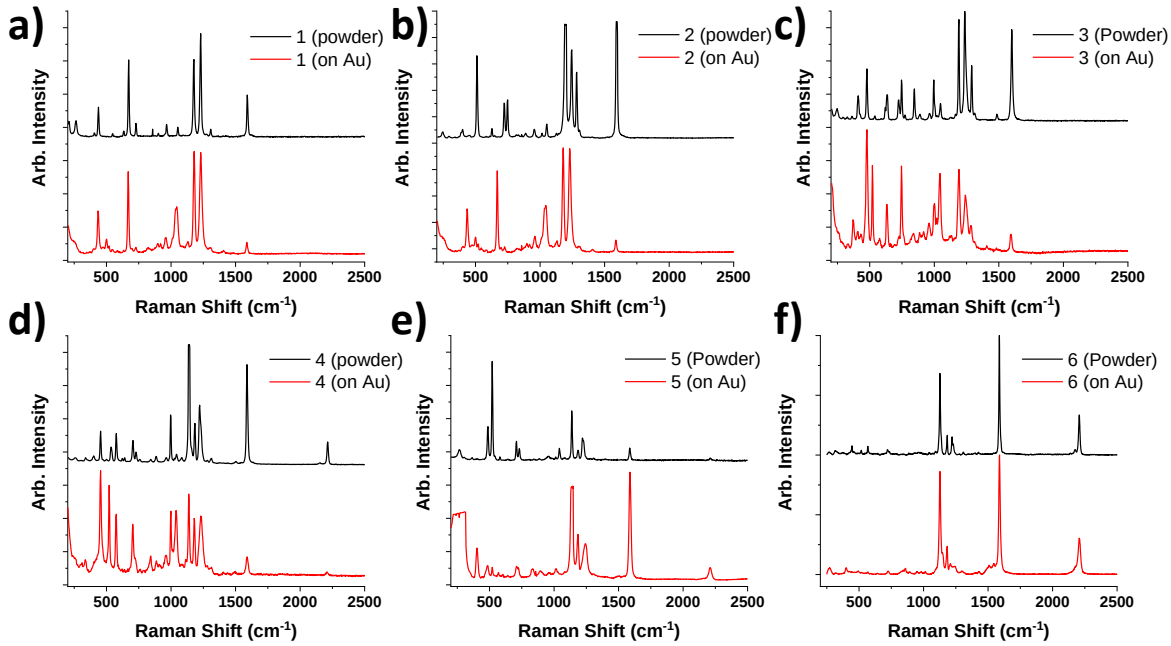

Figure 5. Raman spectroscopy on compounds **1**–**6** as powder on Si substrates and drop-cast (from 1 mM toluene solutions) on to CitAuNPs on silicon substrates. 785 nm laser.

In the Raman data (**Figure 5**), peaks corresponding to vibrational modes of the aromatic backbone of the molecular wires (1600 cm^{-1}) are evident in both the SERS configuration and the powder samples. However, there are some clear changes in relative peak intensities in all examples. For instance, in the spectra for **2**, the peak at 1600 cm^{-1} and the peaks at ≈1150–1250 cm^{-1} have similar relative intensities when acquired directly from the solid-state material. In contrast, spectra for **2** in SERS configuration show the peak at 1600 cm^{-1} with significantly reduced intensity relative to the peaks at ≈1150–1250 cm^{-1}. Such changes in intensity are typical of molecules binding to a surface/being in a different orientation compared to the average orientation in the powder sample, with some modes enhanced by the SERS configuration, and other suppressed due to selection rules. There are several examples across the series of **1–6** where spectra look 'similar' from powder vs. SERS, but nevertheless there are large changes in relative intensities and some subtle shifts in the peaks which are indicative of surface binding. A peak at 1195 cm^{-1} (assigned as C=S stretch)[31] is present throughout all spectra and typically has high

intensity either as powder or drop cast sample. This indicates that the C=S functionality is remaining intact when bound on to the Au particle surface.

GAP mode studies with 2

To further investigate the interaction of the $–CS_2Me$ functionality with the substrate "GAP mode" Raman spectroscopic characterisation has been performed with compound **2** on flame annealed gold slides. GAP mode Raman spectroscopy involves adsorbing gold nanoparticles on top of target monolayers: the plasmonic Au nanoparticles greatly enhance the Raman scattering and allow the recording of good quality spectra from monolayers adsorbed on smooth metal substrates. Gold slides were immersed in a 1 mM toluene solution of **2** for 24 hours and were rinsed thoroughly with toluene. The slide was then immersed in an aqueous solution of AuCitNPs for 1 h,was rinsed with water and methanol, and allowed to dry. Raman results (**Figure 6**) show that despite copious rinsing with solvents that easily dissolve **2**, a strong Raman signature similar to that observed with drop cast solutions was obtained, confirming substantial Raman enhancement in the GAP mode samples. The spectra are generally similar across the nine areas measured in SERS configuration. The peak at 1600 cm^{-1} has a high intensity as an extremely thin layer in the GAP mode measurements, in contrast to the drop cast samples. This suggests an alternative molecular arrangement in the GAP mode measurements compared to bulk measurements on dropcast CitAuNPs. The C=S stretching peak is also present in the GAP mode measurements and is particularly strong in intensity compared to neighbouring peaks.

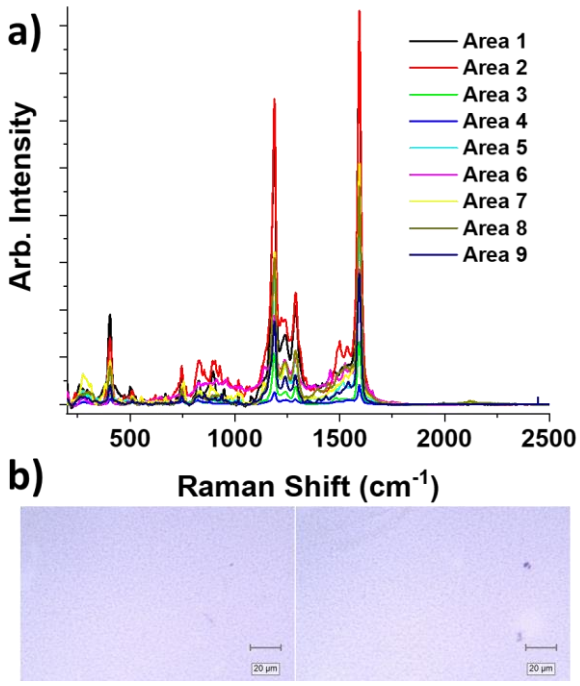

Figure 6. a) Surface enhanced Raman spectrum of GAP mode samples of **2** on gold slides with CitAuNPs. b) Images of gold slides at 50× magnification on confocal microscope showing the array of CitAuNPs fixed on the gold slide by the layer of **2** on the Au surface.

Complexation of Carbodithioate ester with Au^I

The solution stability studies (**Figure 4**) show that the carbodithioate ester functionality remains intact under ambient conditions, but this raises the question: what happens in the presence of Au? To address this, Au^I complex **14** was prepared from commercially available Au^I precursor (**Figure 7**). Analogous ethyl carbodithioate ester complexes have been prepared previously by Butenschön and co-workers for other applications and show the ester remains intact while coordinated to the electron deficient Au^I metal centre.[32]

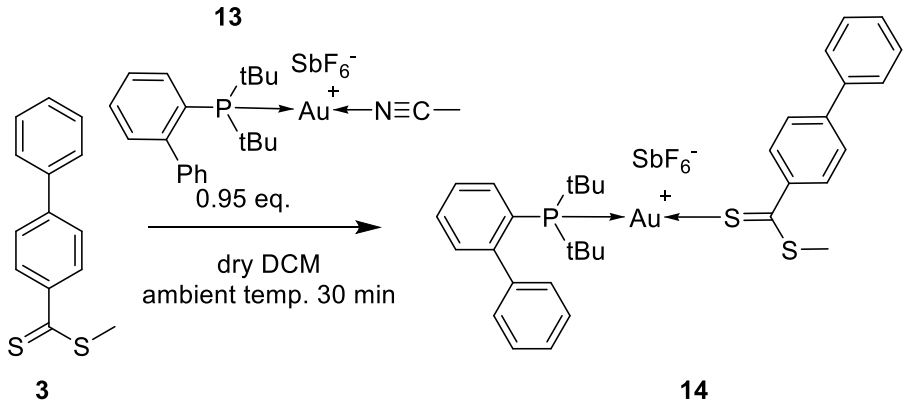

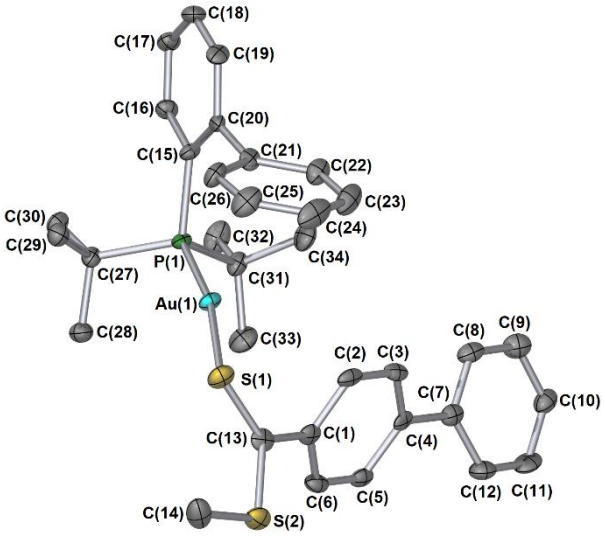

Figure 7 Synthesis of carbodithioate ester-containing Au^I complex **14** (top) and X-ray crystallographic structure of **14** crystallised from DCM/Hexane (bottom). Ellipsoids shown at 50% probablility. Hydrogen atoms and $[SbF_6]^-$ counterion are omitted for clarity.

^{1}H NMR results show clear evidence for the presence of the carbodithioate ester with the S–Me protons at 3.08 ppm, shifted from 2.81 ppm in uncomplexed ligand **3** (See **Figure S5** and **S20**). The electron deficient Au^I center is responsible for this shift upon coordination. The chemical shift of the C=S carbon shifts from 228.9 ppm to 238.8 ppm upon complexation to the Au^I centre.

Crystals of **14** suitable for x-ray diffraction were grown by vapour diffusion from DCM/hexane (**Figure 7**). The X-ray crystallographic structure shows clear evidence for the near linear C=S→Au^{I} interaction. To the best of our knowledge there is no reported X-ray data for such an interaction from a carbodithioate ester (See SI5 for CSD search details). We suggest that this C=S→Au interaction is responsible for the boost in conductance observed in **2** compared to **12**, and that the C=S interaction is likely preferred to the C–SMe→Au interaction. Raman spectroscopy was also performed on **14** as a powder sample (See SI **Figure S25**), which shows a highly similar spectral profile to **3** as powder with the typical C=S stretching peak at 1195 cm^{-1}.

Conclusion

With this study, we have verified the effectiveness of the methyl carbodithioate ester R–CS_2Me as a contact group for gold in molecular electronics. Through a comprehensive, multi-technique study, we have probed its surface and coordination chemistry, its chemical stability, and its charge transport behaviour. We have developed a synthetic protocol that allows the introduction of R-CS_2Me termini in molecular wires through well-known Pd-catalysed C-C cross-coupling reactions. NMR characterisation suggests excellent stability in the presence of water and aerobic oxidants. Raman/SERS and single-crystal XRD data shows excellent resilience of the R–CS_2Me functionality in the presence of aerobic oxidants and metallic substrates. Our initial claim, that R-CS_2Me groups can offer better electrode coupling and more efficient charge transport has been verified by STMBJ measurements, that have unequivocally confirmed the carbodithioate ester being a significantly more transparent electrode contact than widely used alkyl sulfides, while retaining their desirable chemical characteristics.

General Experimental Details

Solvents and reagents: Solvents were dried using an Innovative Technology solvent purification system and were stored in ampules under nitrogen with 3Å molecular sieves. Reagents were obtained from commercial sources and were used without further purification unless specified. Moisture and/or air sensitive experiments were conducted using thoroughly dried glassware under nitrogen atmosphere. Deoxygenation of reactions was performed by bubbling the reaction mixtures using a balloon of argon.

NMR Spectra: ^{1}H-NMR spectra were recorded on a Bruker Avance III HD 500MHz spectrometer. Chemical shifts (δ) in ^{1}H-NMR and ^{13}C-NMR spectra are reported in ppm and were referenced against the residual solvent signal as reported in the literature.[33]

Flash chromatography was carried out on silica gel 60 (40-63 µm) purchased from Merck.

Mass spectra: High resolution mass spectrometry for **5** and **6** was carried out on a Waters LCT Premier XE using ASAP ionization with TOF detection. Samples were analyzed directly as solids. All other HRMS was performed on an Agilent 7200 Q-TOF instrument.

Citrate capped gold nanoparticles for deposition on to silicon wafers were prepared using literature procedures [30] with slight modifications. 100 mL of 0.01% $HAuCl_4$ (aq) was raised to boiling temperature with vigorous stirring and adding 0.7 mL of 1% sodium citrate (aq) solution and continuing reflux for 30 minutes. The resulting solution was centrifuged in 50 mL falcon tubes at 4000 rpm for 5 hours, and the supernatant was carefully removed leaving ≈ 1 mL of particle stock solution. This solution was dropped on to silicon wafers and dried in an oven at 80 °C overnight. Solutions of carbodithioate ester analyte were drop-cast on these samples from 1 mM toluene solutions as required.

Raman spectroscopy was performed on a B&W Tek Mini-Ram II with 10 s integration time using a 785 nm laser. The laser power was varied on this instrument to obtain the best signal without degrading the sample and minimizing any fluorescence.

GAP Mode Raman Microscopy was performed on an inVia Reflex Qontor Confocal Raman Microscope using a 785 nm laser on 1% laser power with 10 separate 1 second acquisitions.

Synthesis and Characterization is available in the supporting information.

ASSOCIATED CONTENT

Supporting information is attached as part of this submission.

Raw data is available at https://datacat.liverpool.ac.uk/id/eprint/2481

DOI: 10.17638/datacat.liverpool.ac.uk/2481

Acknowledgments

This work was supported with funding from the Leverhulme Foundation (grant RPG-2019-308). A.V. Acknowledges funding from the Royal Society (URF\R1\191241). Dr Nathan Halcovitch is thanked for guidance with the WebCSD search. Durham University Chemistry is thanked for in-kind mass spectrometry measurements of **5** and **6** by ASAP-TOF.

References

(1) Tang, C.; Ayinla, R. T.; Wang, K. Beyond electrical conductance: progress and prospects in single-molecule junctions. *J. Mater. Chem. C* **2022**, *10*, 13717-13733.

(2) Ward, J. S.; Vezzoli, A. Key advances in electrochemically-addressable single-molecule electronics. *Curr. Opin. Electrochem.* **2022**, *35*, 101083.

(3) Tan, Z.; Jiang, W.; Tang, C.; Chen, L.-C.; Chen, L.; Liu, J.; Liu, Z.; Zhang, H.-L.; Zhang, D.; Hong, W. The Control of Intramolecular Through-Bond and Through-Space Coupling in Single-Molecule Junctions. *CCS Chemistry* **2021**, *4*, 713-721.

(4) Lv, S.-L.; Zeng, C.; Yu, Z.; Zheng, J.-F.; Wang, Y.-H.; Shao, Y.; Zhou, X.-S. Recent Advances in Single-Molecule Sensors Based on STM Break Junction Measurements. *Biosensors* **2022**, *12*, 565.

(5) Miyazaki, T.; Shoji, Y.; Fujii, S.; Fukushima, T. A single-molecule conductance study on the rotational isomers of a hexaarylbenzene derivative carrying dipolar rotating units. *Jpn J. Appl. Phys.* **2021**, *60*, 108002.

(6) Chen, F.; Hihath, J.; Huang, Z.; Li, X.; Tao, N. J. Measurement of Single-Molecule Conductance. *Annu. Rev. Phys. Chem.* **2007**, *58*, 535-564.

(7) Su, T. A.; Neupane, M.; Steigerwald, M. L.; Venkataraman, L.; Nuckolls, C. Chemical principles of single-molecule electronics. *Nat. Rev. Mater.* **2016**, *1*, 16002.

(8) Daaoub, A.; Morris, J. M. F.; Béland, V. A.; Demay-Drouhard, P.; Hussein, A.; Higgins, S. J.; Sadeghi, H.; Nichols, R. J.; Vezzoli, A.; Baumgartner, T.; Sangtarash, S. Not So Innocent After All: Interfacial Chemistry Determines Charge-Transport Efficiency in Single-Molecule Junctions. *Angew. Chem. Int. Ed.* **2023**, *62*, e202302150.

(9) Chen, F.; Li, X.; Hihath, J.; Huang, Z.; Tao, N. Effect of Anchoring Groups on Single-Molecule Conductance: Comparative Study of Thiol-, Amine-, and Carboxylic-Acid-Terminated Molecules. *J. Am. Chem. Soc.* **2006**, *128*, 15874-15881.

(10) van Veen, F. H.; Ornago, L.; van der Zant, H. S. J.; El Abbassi, M. Benchmark Study of Alkane Molecular Chains. *J. Phys. Chem. C.* **2022**, *126*, 8801-8806.

(11) Xie, Z.; Bâldea, I.; Oram, S.; Smith, C. E.; Frisbie, C. D. Effect of Heteroatom Substitution on Transport in Alkanedithiol-Based Molecular Tunnel Junctions: Evidence for Universal Behavior. *ACS Nano* **2017**, *11*, 569-578.

(12) Xie, Z.; Bâldea, I.; Frisbie, C. D. Energy Level Alignment in Molecular Tunnel Junctions by Transport and Spectroscopy: Self-Consistency for the Case of Alkyl Thiols and Dithiols on Ag, Au, and Pt Electrodes. *J. Am. Chem. Soc.* **2019**, *141*, 18182-18192.

(13) Xue, Y.; Li, X.; Li, H.; Zhang, W. Quantifying thiol–gold interactions towards the efficient strength control. *Nat. Commun.* **2014**, *5*, 4348.

(14) Bürgi, T. Properties of the gold–sulphur interface: from self-assembled monolayers to clusters. *Nanoscale* **2015**, *7*, 15553-15567.

(15) Leary, E.; La Rosa, A.; González, M. T.; Rubio-Bollinger, G.; Agraït, N.; Martín, N. Incorporating single molecules into electrical circuits. The role of the chemical anchoring group. *Chem. Soc. Rev.* **2015**, *44*, 920-942.

(16) Park, Y. S.; Whalley, A. C.; Kamenetska, M.; Steigerwald, M. L.; Hybertsen, M. S.; Nuckolls, C.; Venkataraman, L. Contact Chemistry and Single-Molecule Conductance: A Comparison of Phosphines, Methyl Sulfides, and Amines. *J. Am. Chem. Soc.* **2007**, *129*, 15768-15769.

(17) Gantenbein, M.; Li, X.; Sangtarash, S.; Bai, J.; Olsen, G.; Alqorashi, A.; Hong, W.; Lambert, C. J.; Bryce, M. R. Exploring antiaromaticity in single-molecule junctions formed from biphenylene derivatives. *Nanoscale* **2019**, *11*, 20659-20666.

(18) Davidson, R.; Al-Owaedi, O. A.; Milan, D. C.; Zeng, Q.; Tory, J.; Hartl, F.; Higgins, S. J.; Nichols, R. J.; Lambert, C. J.; Low, P. J. Effects of Electrode–Molecule Binding and Junction Geometry on the Single-Molecule Conductance of bis-2,2′:6′,2″-Terpyridine-based Complexes. *Inorg. Chem.* **2016**, *55*, 2691-2700.

(19) Kaliginedi, V.; V. Rudnev, A.; Moreno-García, P.; Baghernejad, M.; Huang, C.; Hong, W.; Wandlowski, T. Promising anchoring groups for single-molecule conductance measurements. *Phys. Chem. Chem. Phys* **2014**, *16*, 23529-23539.

(20) Moreno-García, P.; Gulcur, M.; Manrique, D. Z.; Pope, T.; Hong, W.; Kaliginedi, V.; Huang, C.; Batsanov, A. S.; Bryce, M. R.; Lambert, C.; Wandlowski, T. Single-Molecule Conductance of

Functionalized Oligoynes: Length Dependence and Junction Evolution. *J. Am. Chem. Soc.* **2013**, *135*, 12228-12240.

(21) Liu, J.; Zhao, X.; Al-Galiby, Q.; Huang, X.; Zheng, J.; Li, R.; Huang, C.; Yang, Y.; Shi, J.; Manrique, D. Z.; Lambert, C. J.; Bryce, M. R.; Hong, W. Radical-Enhanced Charge Transport in Single-Molecule Phenothiazine Electrical Junctions. *Angew. Chem. Int. Ed.* **2017**, *56*, 13061-13065.

(22) Ozawa, H.; Baghernejad, M.; Al-Owaedi, O. A.; Kaliginedi, V.; Nagashima, T.; Ferrer, J.; Wandlowski, T.; García-Suárez, V. M.; Broekmann, P.; Lambert, C. J.; Haga, M.-a. Synthesis and Single-Molecule Conductance Study of Redox-Active Ruthenium Complexes with Pyridyl and Dihydrobenzo[b]thiophene Anchoring Groups. *Chem. Eur. J.* **2016**, *22*, 12732-12740.

(23) Chen, W.; Li, H.; Widawsky, J. R.; Appayee, C.; Venkataraman, L.; Breslow, R. Aromaticity Decreases Single-Molecule Junction Conductance. *J. Am. Chem. Soc.* **2014**, *136*, 918-920.

(24) Li, Z.; Li, H.; Chen, S.; Froehlich, T.; Yi, C.; Schönenberger, C.; Calame, M.; Decurtins, S.; Liu, S.-X.; Borguet, E. Regulating a Benzodifuran Single Molecule Redox Switch via Electrochemical Gating and Optimization of Molecule/Electrode Coupling. *J. Am. Chem. Soc.* **2014**, *136*, 8867-8870.

(25) Zhao, H.; Wang, J.; Zheng, Y.; Li, J.; Han, X.; He, G.; Du, Y. Organic Thiocarboxylate Electrodes for a Room-Temperature Sodium-Ion Battery Delivering an Ultrahigh Capacity. *Angew. Chem. Int. Ed.* **2017**, *56*, 15334-15338.

(26) Querner, C.; Benedetto, A.; Demadrille, R.; Rannou, P.; Reiss, P. Carbodithioate-Containing Oligo- and Polythiophenes for Nanocrystals' Surface Functionalization. *Chem. Mater.* **2006**, *18*, 4817-4826.

(27) Xu, B.; Tao, N. J. Measurement of Single-Molecule Resistance by Repeated Formation of Molecular Junctions. *Science* **2003**, *301*, 1221-1223.

(28) Wu, C.; Bates, D.; Sangtarash, S.; Ferri, N.; Thomas, A.; Higgins, S. J.; Robertson, C. M.; Nichols, R. J.; Sadeghi, H.; Vezzoli, A. Folding a Single-Molecule Junction. *Nano Lett.* **2020**, *20*, 7980-7986.

(29) Barden, W. R. T.; Singh, S.; Kruse, P. Roughening of Gold Atomic Steps Induced by Interaction with Tetrahydrofuran. *Langmuir* **2008**, *24*, 2452-2458.

(30) Li, J. F.; Tian, X. D.; Li, S. B.; Anema, J. R.; Yang, Z. L.; Ding, Y.; Wu, Y. F.; Zeng, Y. M.; Chen, Q. Z.; Ren, B.; Wang, Z. L.; Tian, Z. Q. Surface analysis using shell-isolated nanoparticle-enhanced Raman spectroscopy. *Nat. Protoc.* **2013**, *8*, 52-65.

(31) Storer, A. C.; Ozaki, Y.; Carey, P. R. Resonance Raman spectroscopic evidence for an intramolecular interaction involving the amide and dithioester groups of N-acyl glycine ethyl dithioesters. *Can. J. Chem.* **1982**, *60*, 199-209.

(32) Schmiel, S.-F.; Butenschön, H. New π-Extended 1,1′-Disubstituted Ferrocenes with Thioate and Dithioate End Groups. *Eur. J. Org .Chem.* **2021**, *2021*, 2388-2401.

(33) Fulmer, G. R.; Miller, A. J. M.; Sherden, N. H.; Gottlieb, H. E.; Nudelman, A.; Stoltz, B. M.; Bercaw, J. E.; Goldberg, K. I. NMR Chemical Shifts of Trace Impurities: Common Laboratory Solvents, Organics, and Gases in Deuterated Solvents Relevant to the Organometallic Chemist. *Organometallics* **2010**, *29*, 2176-2179.